Xenopus oocyte meiosis lacks spindle assembly checkpoint control

Hua Shao,[1] Ruizhen Li,[1] Chunqi Ma,[1] Eric Chen,[1] and X. Johné Liu[1,2,3]

[1]Ottawa Hospital Research Institute, The Ottawa Hospital, Ottawa, Ontario K1H BL6, Canada
[2]Department of Obstetrics and Gynaecology, and [3]Department of Biochemistry, Microbiology and Immunology, University of Ottawa, Ottawa, Ontario K1N 6N5, Canada

The spindle assembly checkpoint (SAC) functions as a surveillance mechanism to detect chromosome misalignment and to delay anaphase until the errors are corrected. The SAC is thought to control mitosis and meiosis, including meiosis in mammalian eggs. However, it remains unknown if meiosis in the eggs of nonmammalian vertebrate species is also regulated by SAC. Using a novel karyotyping technique, we demonstrate that complete disruption of spindle microtubules in *Xenopus laevis* oocytes did not affect the bivalent-to-dyad transition at the time oocytes are undergoing anaphase I. These oocytes also acquired the ability to respond to parthenogenetic activation, which indicates proper metaphase II arrest. Similarly, oocytes exhibiting monopolar spindles, via inhibition of aurora B or Eg5 kinesin, underwent monopolar anaphase on time and without additional intervention. Therefore, the metaphase-to-anaphase transition in frog oocytes is not regulated by SAC.

Introduction

In mitosis, the spindle assembly checkpoint (SAC) functions as a surveillance mechanism to detect chromosome misalignment and to delay anaphase initiation until the errors are corrected (Musacchio and Salmon, 2007). Upon satisfying bipolar attachment of all chromosomes, anaphase initiation is thought to be brought about by the activation of anaphase-promoting complex/cyclosome (APC/C, or simply APC), an E3 ligase that targets cyclin B and securin, among many other protein substrates, for proteolysis (Pines, 2006). Securin degradation leads to activation of separase and removal of cohesin, thus releasing sister chromatids. Degradation of cyclin B results in the inactivation of cyclin-dependent kinase 1 (CDK1), allowing mitotic exit with ensuing anaphase and cytokinesis (Pines, 2006).

Kinetochore–microtubule interaction is thought to be key in SAC regulation (Rieder et al., 1994, 1995). In prometaphase, major SAC proteins MAD2, BUBR1/Mad3, and BUB3 form the mitotic checkpoint complex (MCC) at kinetochores. Kinetochore-associated MCC binds and sequesters a key APC activator Cdc20. Cdc20 sequestration at kinetochores prevents APC activation. Many other SAC proteins including BUB1 and MAD1 are thought to serve this central scheme by either facilitating MCC assembly at kinetochores or propagating Cdc20 sequestration. At metaphase when sister kinetochores are fully occupied by kinetochore microtubules and are bioriented, MCC become dissociated from kinetochores, releasing Cdc20 which in turn activates APC (Musacchio and Salmon, 2007).

A functional SAC is clearly present in mouse oocytes undergoing meiosis. This is best supported by studies involving high concentrations of nocodazole. Hence, complete disruption of meiosis I spindle by nocodazole causes metaphase I arrest with intact chromosome bivalents; upon nocodazole removal, the oocyte reforms the metaphase I spindle and proceeds to anaphase and cytokinesis to emit the first polar body (Wassarman et al., 1976; Schultz and Wassarman, 1977; Eichenlaub-Ritter and Boll, 1989; Soewarto et al., 1995; Brunet et al., 1999; Homer et al., 2005). However, strict bipolar attachment of chromosomes at the metaphase plane is not required for anaphase initiation in mouse oocytes (LeMaire-Adkins et al., 1997; Nagaoka et al., 2011; Kolano et al., 2012), which suggests that the SAC in mouse oocytes may be less stringent than in mitosis.

However, it remains unknown if meiosis in the oocytes of nonmammalian vertebrate species is also regulated by SAC. Progesterone triggers the resumption of meiosis in *Xenopus*

H. Shao and R. Li contributed equally to this paper.

Correspondence to X. Johné Liu: jliu@ohri.ca

Abbreviations used in this paper: APC, anaphase-promoting complex/cyclosome; Aur-B, aurora B; GVBD, germinal vesicle breakdown; MCC, mitotic checkpoint complex; OCM, oocyte culture medium; OR2, oocyte incubation medium; SAC, spindle assembly checkpoint; STLC, S-trityl L-cysteine.

The Rockefeller University Press $30.00
J. Cell Biol. Vol. 201 No. 2 191–200
www.jcb.org/cgi/doi/10.1083/jcb.201211041

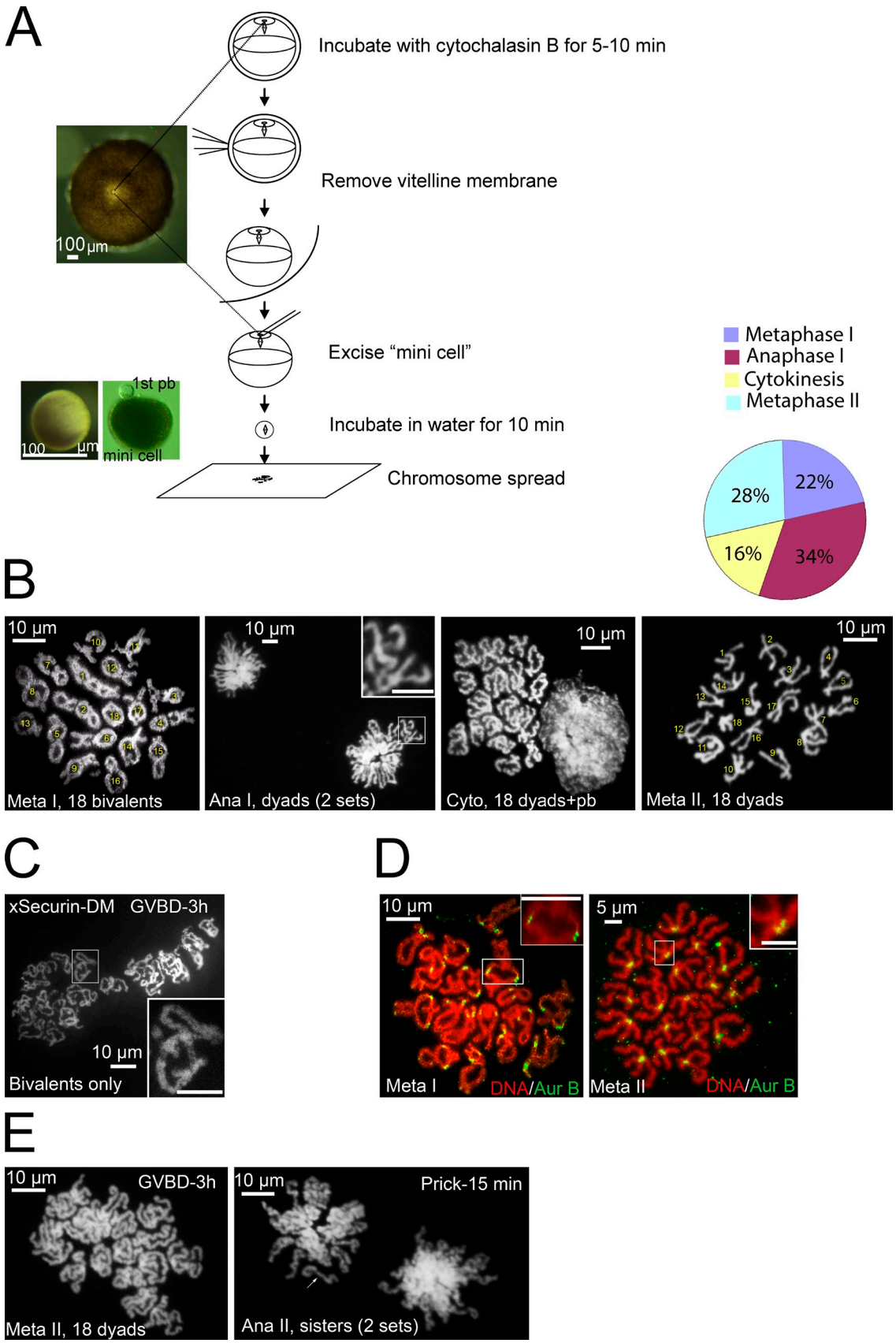

Figure 1. **Karyotyping *Xenopus* oocytes during meiosis.** (A) Schematic illustration of karyotyping *Xenopus* oocytes: two mini-cells are shown, one without a polar body (left, with overhead light) and the other with a first polar body (pb) still attached (right, photographed with transmission light). (B) Representative images of oocytes at metaphase I, anaphase I, cytokinesis, and metaphase II. The graph summarizes karyotypes of 94 oocytes (>10 experiments) analyzed between 115 and 145 min after GVBD. Numbers are used to facilitate chromosome counting, not to imply chromosome identities. The inset

laevis oocytes through a nongenomic mechanism (Bayaa et al., 2000; Tian et al., 2000), activating a cascade of signaling events leading to the abrupt activation of MAP kinase (Ferrell and Machleder, 1998; Ohan et al., 1999), concurrent with germinal vesicle breakdown (GVBD). Accompanying full MAP kinase activation is also the full activation of CDK1, as well as hyperphosphorylation of Cdc20, which is suggestive of APC activation (Taieb et al., 2001; Ma et al., 2006). Shortly after GVBD, partial cyclin B degradation is noticeable such that by 1 h after GVBD, the level has reduced by >50%, before the level starts to rise again (Ma et al., 2003; Belloc and Méndez, 2008). Furthermore, metaphase-to-anaphase transition occurs 2 h after GVBD, at a time when the cyclin B level (and CDK1 activity) has started to rise after the transient and partial drop (Furuno et al., 1994; Ohsumi et al., 1994; Ma et al., 2006). Perhaps not surprisingly, inhibition of APC, via interfering with the function of the APC activator Cdc20 or APC core subunit Cdc27, prevents cyclin B degradation but does not prevent frog oocytes from completing meiosis I or metaphase II arrest (Peter et al., 2001; Taieb et al., 2001).

The timing of Cdc20 hyperphosphorylation and partial degradation of cyclin B clearly indicate that these events are not controlled by a spindle-based mechanism. However, this does not necessarily mean that anaphase initiation in frog oocytes is not regulated by SAC. Direct determination of SAC requires disruption of meiotic spindles followed by assessing meiotic chromosome progression, and/or by assessing if, upon spindle reassembly, the oocytes spontaneously resume meiosis I to emit the first polar body. None of this has been accomplished in oocytes of any nonmammalian species. In *Xenopus* oocytes, it is hampered by the inability of karyotyping meiotic chromosomes after nuclear envelop breakdown, and by the apparent irreversibility of the microtubule poison nocodazole in intact oocytes. We have overcome both obstacles in this study in a direct examination of SAC function in frog oocyte meiosis.

Results and discussion

Developing a novel karyotyping technique to analyze frog chromosomes during meiosis

Although lampbrush chromosome bivalents have been observed in prophase oocytes by first isolating the nucleus (germinal vesicle; Gall and Wu, 2010), this method is not applicable after GVBD or during meiosis I–to–meiosis II transition. Taking advantage of the fact that spindle assembly and polar body emission take place at the animal pole cortex with a clearly visible spindle attachment site (Fig. 1 A), we excised a "mini-cell" (80–100 µm) containing the spindle, and subjected it to chromosome spreading. Fig. 1 B shows the typical image of *Xenopus* chromosomes at metaphase I, anaphase I, cytokinesis, and metaphase II, respectively. The metaphase I spread consists of 18 (Graf and Kobel, 1991) clearly identifiable chromosome bivalents. These bivalents resembled the lampbrush bivalents of prophase oocytes (Gall and Wu, 2010), with the exception that the condensed metaphase I bivalents appeared much more compact (∼10 µm across the long axis; Fig. 1 B, Meta I) than the lampbrush bivalents (∼100 µm; Gall and Wu, 2010). Metaphase II oocytes contained 18 metacentric chromosome dyads (Fig. 1 B, Meta II; Graf and Kobel, 1991). Mini cells derived from anaphase I oocytes exhibit two sets of segregating dyads (Fig. 1 B, Ana I). Mini-cells derived from oocytes at a late stage of cytokinesis had 18 dyads alongside an aggregated chromosome mass indicative of polar body chromatin (Fig. 1 B, Cyto), which indicates that the polar body was still attached to the mini-cell (see Fig. 1 A, right mini-cell), suggesting that abscission was not complete. The graph in Fig. 1 B summarizes our karyotype analyses of oocytes 115–145 min after GVBD (at the time of bursting the mini-cell onto the glass slide). We did not find any oocytes that contained a mixture of bivalents and dyads, which indicates that chromosome segregation was synchronous, consistent with observation in live cell imaging (Zhang et al., 2008; Shao et al., 2012; also see Fig. 4 A, top).

To eliminate any possibility that the karyotyping technique may cause unintended chromosome changes, we analyzed oocytes injected with mRNA coding xSecurin-DM, which inhibits separase activation (Zou et al., 1999; Zhang et al., 2008) and blocks chromosome segregation in meiosis I (Zhang et al., 2008). As expected, all xSecurin-DM oocytes (11/11, two experiments) analyzed 3 h after GVBD contained only bivalent chromosomes, although the bivalents were somewhat more relax and "twisted" (Fig. 1 C) than those found at metaphase I in control oocytes. These results, and those in our earlier study (Zhang et al., 2008), clearly indicate that anaphase I in frog oocytes requires separase-mediated cohesin degradation, contrary to the claim of an earlier study (Peter et al., 2001).

To further characterize bivalent and dyad chromosomes, we immunostained metaphase I and metaphase II chromosome spreads with antibodies against aurora B (Aur-B), a centromeric protein (Zhang et al., 2008). In metaphase I spreads, Aur-B was most prominently seen at the two homologous centromere loci, each consisting of two sister centromeres (Fig. 1 D, Meta I, inset). In metaphase II spreads, Aur-B was associated with the two sister centromeres (Fig. 1 D, Meta II, inset).

Making mini-cells after parthenogenetic activation (pricking with a fine glass needle, mimicking fertilization) of metaphase II eggs (Leblanc et al., 2011) was much more challenging due to the significant surface contraction, which often prevented the mini-cell

shows two dyads. (C) A representative karyotype image of oocytes injected with xSecurin-DM mRNA at 3 h after GVBD. The inset depicts a single bivalent. (D) Metaphase I (left) and metaphase II (right) chromosome spreads double-stained with Sytox orange and anti–Aur-B. In metaphase I spread, each bivalent (inset) has two pairs of Aur-B foci representing two maternal and two paternal sister centromeres, respectively. In metaphase II spread, each dyad (inset) has two closely associated Aur-B foci representing the two sister centromeres. (E) Metaphase II oocytes before (left) and 15 min after (right) prick activation ($n = 7$). Note that metaphase II chromosome dyads in these oocytes have more elongated arms than those shortly after polar body emission (see B). Anaphase II spread consists of two sets of sister chromatids (arrow). Bars: (insets) 10 µm.

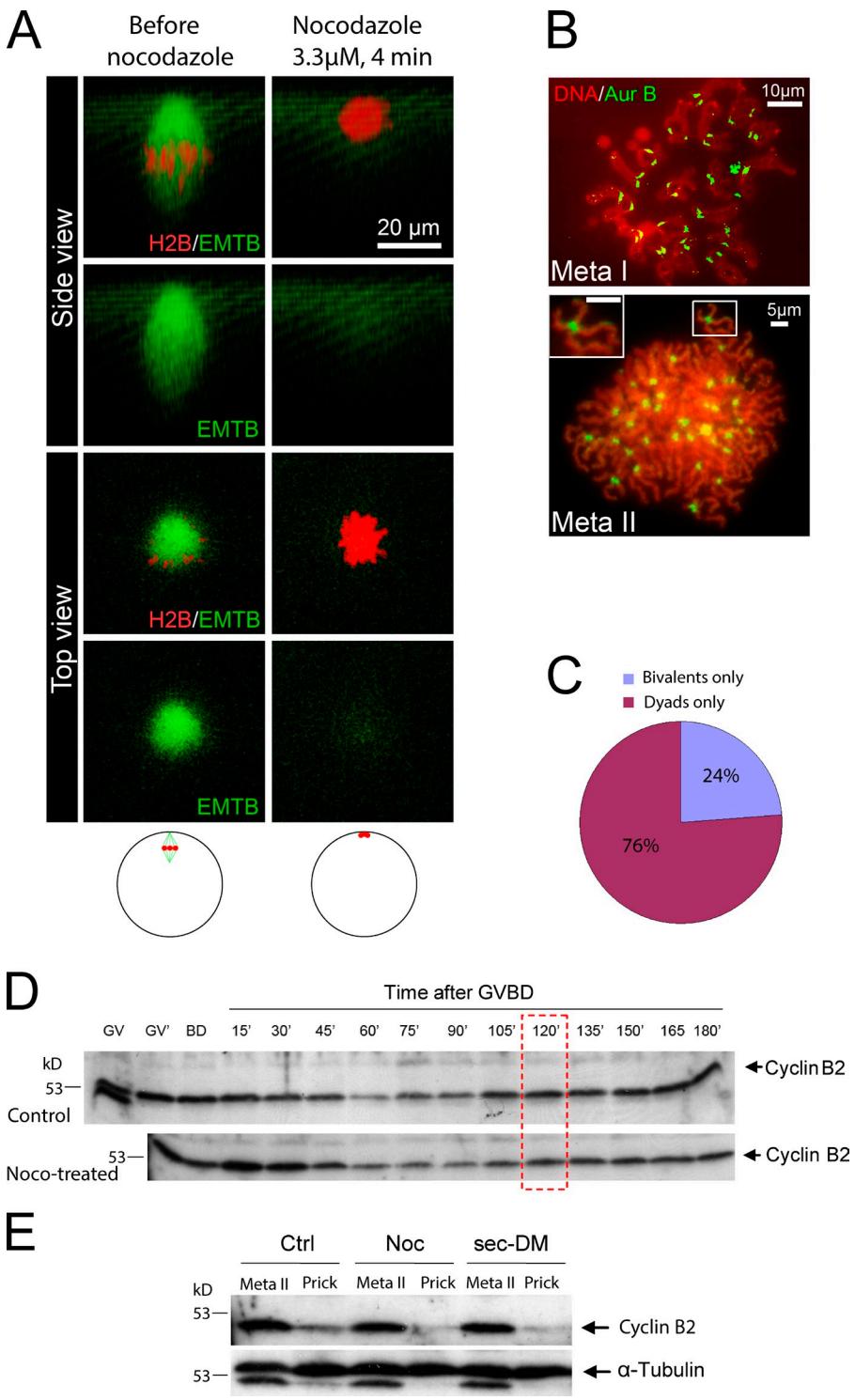

Figure 2. **Bivalent-to-dyad transition in the absence of spindle microtubules.** (A) An oocyte injected with mChe-H2B and EMTB-3GFP was imaged 1 h after GVBD (left). Nocodazole was added to the imaging well (3.3 μM in OR2), followed by time-lapse imaging for >2 h. Shown on the right are images 4 min after the addition of nocodazole. The schematic depicts the position of spindle/chromosomes in live oocyte before (left) and after (right) nocodazole treatment. See Video 1 for the entire series. The images are representative of three movies. (B) 1 h after GVBD, the oocytes were placed in OR2 plus 3.3 μM nocodazole. Oocytes were karyotyped in the presence of 3.3 μM nocodazole such that the mini-cells burst onto glass slides either <100 min after GVBD (metaphase I) or 3 h after GVBD (metaphase II, inset showing one dyad). The slides were stained with Sytox orange and anti–Aur-B. (C) Oocytes were treated as described in B, except that all oocytes were karyotyped between 110 and 130 min after GVBD. The graph summarizes three experiments ($n = 25$). (D) Control oocytes, or oocytes treated with nocodazole, were lysed individually at germinal vesicles (no progesterone) 2 h after the addition of progesterone but before GVBD (GV'), at GVBD (BD), or at the indicated time after GVBD. Extracts were immunoblotted with anti–cyclin B2. Each lane represents half the extract from one oocyte. The red box indicates time of metaphase I–to–anaphase I transition in frog oocytes. Data are representative of three experiments. (E) Control oocytes, nocodazole-treated oocytes (from GVDB, 1 h), and oocytes injected with xSecurin-DM mRNA were selected individually at 3 h after GVBD. The oocytes were either lysed immediately (metaphase II) or 10 min after being pricked. The resulting extracts were subjected to immunoblotting with anti–cyclin B2, followed by anti–α-tubulin of the same membrane. Note the residual cyclin B2 signal on the α-tubulin blot. Data shown are representative of five experiments.

from sealing. Nonetheless, we succeeded in capturing a few mini-cells containing both sets of anaphase II sister chromatids (Fig. 1 E, arrow; compared with dyads in anaphase I spreads shown in Fig. 1 B).

Nocodazole did not interfere with the timing of bivalent-to-dyad transition or global cyclin B degradation

Treating frog oocytes with as little as 100 nM nocodazole disrupts bipolar spindles and inhibits polar body emission (Leblanc et al., 2011). To effect complete microtubule destruction, we added 3.3 μM nocodazole (1 mg/ml) 1 h after GVBD (when a bipolar meiosis I spindle is seen perpendicular to the animal pole cortex; Fig. 2 A). Within 4 min of the addition of nocodazole, the spindles completely disappeared (Fig. 2 A; see Fig. S1 for experiments in which we used anti-tubulin antibodies to detect microtubules in fixed oocytes). Accompanying the disappearance of spindle microtubules, chromosomes appeared to aggregate to the cortex and thereafter remained

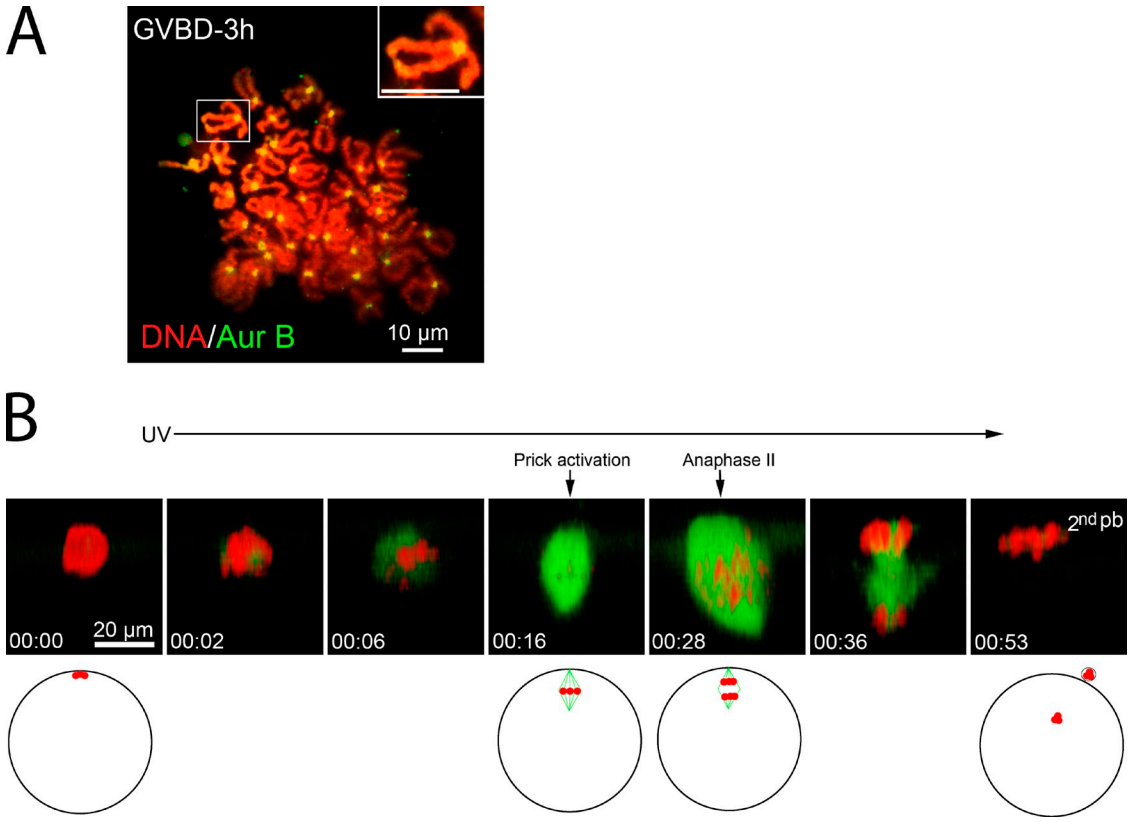

Figure 3. **Colcemid-treated oocytes are arrested in metaphase II.** (A) A representative colcemid-treated (50 µM) oocyte karyotyped 3 h after GVBD, stained with Sytox orange and anti–Aur-B (n = 9). The inset depicts a single dyad. (B) A colcemid-treated (50 µM) oocyte was imaged live, beginning at 3 h after GVBD (00:00). The oocyte was then exposed to UV excitation until the end of the imaging experiment. The oocyte was pricked immediately after the scan at 00:16. The schematic depicts position of the spindle/chromosomes in a live oocyte. Note that the egg chromosomes at 00:53 would be forming the female pronucleus and be beyond the depth of the confocal imaging system. See Video 2 for the entire series.

relatively unchanged for an extended period of time (Fig. 2 A and Video 1). Upon removal of nocodazole, no spindles could be seen, even after overnight incubation in nocodazole-free medium (not depicted). To determine if nocodazole treatment arrested frog oocytes in metaphase I, we karyotyped oocytes after complete spindle destruction. 30–40 min after the addition of nocodazole (or 90–100 min after GVBD), oocytes chromosomes remained as bivalents (Fig. 2 B, top; 18/18), as did control oocytes at the same stage (Fig. 1, B and D). Oocytes analyzed in metaphase II (at least 3 h after GVBD, 22/22) contained ∼36 chromosome dyads (Fig. 2 B, bottom; based on the number of Aur-B foci, each consisting of a pair of sister centromeres), which indicates that bivalent-to-dyad transition had occurred in the absence of microtubules. Analyzing oocytes between 110 and 130 min after GVBD found either uniform bivalents or uniform dyads, but no oocytes that contained a mixture of bivalents and dyads (Fig. 2 C). These results indicate that, like in control oocytes, bivalent-to-dyad transition in the absence of spindle microtubules was also synchronous and on time (∼120 min after GVBD). This is in contrast to nocodazole-treated mouse oocytes, which arrest at metaphase I with bivalent chromosomes and which resume meiosis and emit the first polar body upon drug removal (Wassarman et al., 1976; Soewarto et al., 1995; Homer et al., 2005; Fig. S2).

Nocodazole treatment did not alter the partial degradation and resynthesis of cyclin B during oocyte maturation (Fig. 2 D; n = 3). Although nocodazole-treated oocytes do not recover spindle upon drug removal, these oocytes were capable of responding to parthenogenetic activation to exhibit surface contraction (not depicted) and rapid cyclin B degradation (Fig. 2 E; n = 5), similar to control oocytes and oocytes injected with xSecurin-DM, which indicates that a spindle is not required to elicit cyclin B degradation after parthenogenetic activation. These results suggest that meiosis II is similarly not regulated by SAC.

Frog oocytes proceed to metaphase II arrest in the absence of spindle microtubules

These results indicated that nocodazole-treated frog oocytes successfully completed bivalent-to-dyad transition, suggesting that these oocytes were arrested at metaphase II. However, the lack of spindle reformation upon nocodazole removal had precluded the direct confirmation that these were truly metaphase II eggs capable of responding to parthenogenetic activation to emit the second polar body (Leblanc et al., 2011). To circumvent this, we used colcemid, a UV-labile microtubule-disrupting drug (Sluder, 1979). As expected, the presence of 50 µM colcemid during oocyte maturation did not interfere with GVBD (not depicted). When oocytes were karyotyped 3 h after GVBD, all contained only chromosome dyads (Fig. 3 A), which indicates that these oocytes had similarly completed

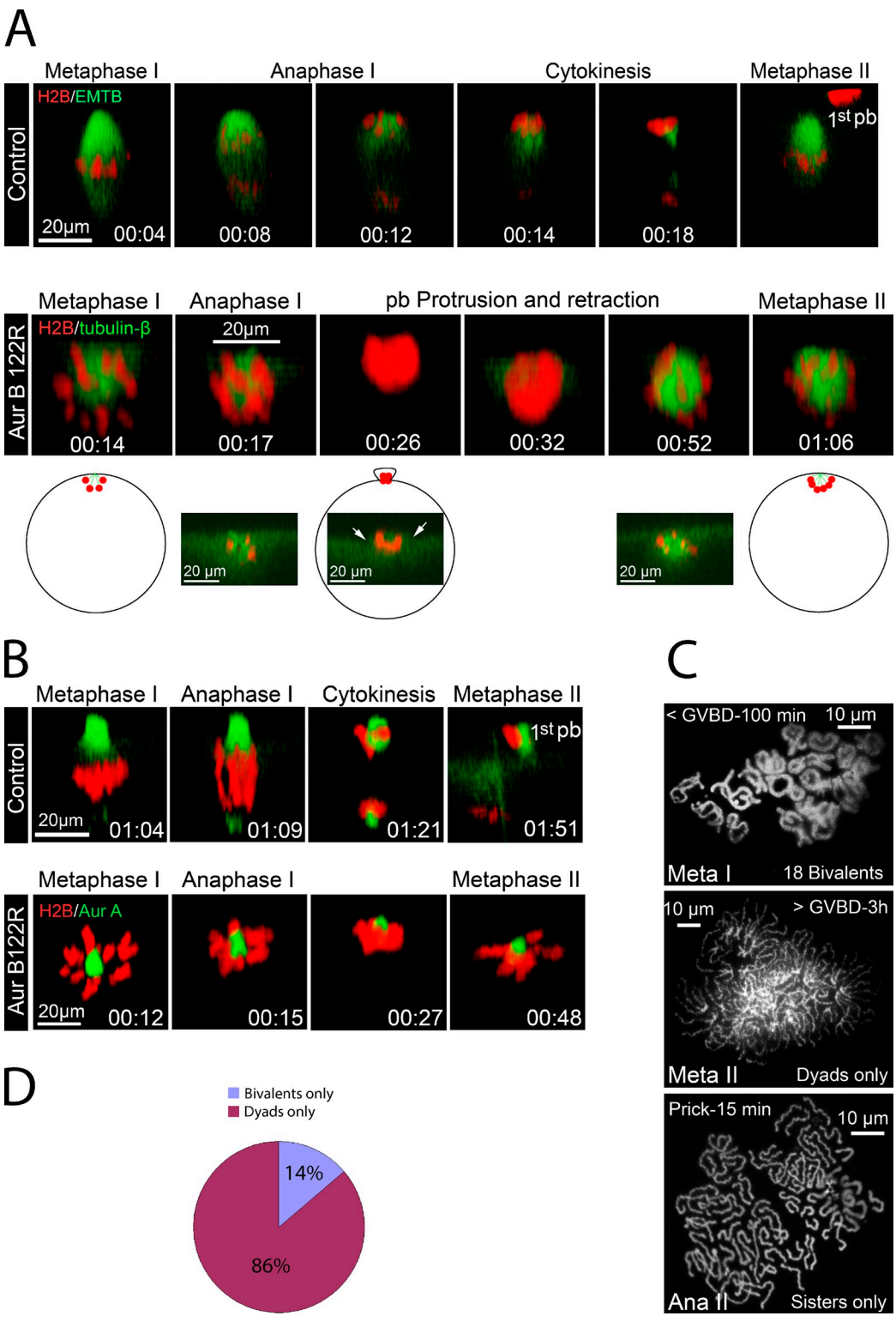

Figure 4. **Monopolar Aur-B122R oocytes underwent anaphase I and anaphase II.** (A, top) Time series (side view) of a representative oocyte injected with wild-type Aur-B (as control), depicting metaphase I (00:04), anaphase I (00:08 and 00:12), and cytokinesis (00:14 and 00:18). See Video 3 for the entire series. The far right image (metaphase II) was from a different oocyte in the same experiment. (A, bottom) Time series (side view) of a representative Aur-B122R mRNA-injected oocyte exhibiting a monopolar spindle (00:14), monopolar anaphase (00:17 and 00:26), and metaphase II with another monopolar spindle (01:06). Cross-sectional views of selective time points are also shown to depict the transient membrane protrusion (00:26, arrows). The schematic depicts the position of the monopolar spindle/chromosomes in live oocyte. See Video 4 for the entire series (n = 9). (B, top) Time series (side view) of a control oocyte undergoing meiosis I, via imaging chromosomes (H2B) and the spindle poles (Alexa Fluor 488 anti–Aur-A). See Video 5 for the entire series (n = 9). (B, bottom) Time series (side view) of a representative monopolar Aur-B122R oocyte, depicting chromosome poleward movement (00:15 and 00:27) followed by the formation of another monopolar (meiosis II) spindle (00:48). See Video 6 for the entire series (n = 13). (C) Karyotype analyses of monopolar Aur-B122R oocytes at metaphase I (top), metaphase II (middle), and 15 min after prick activation (bottom). (D) Monopolar Aur-B122R oocytes were karyotyped between 110 and 145 min after GVBD. The graph summarizes >10 experiments (n = 72).

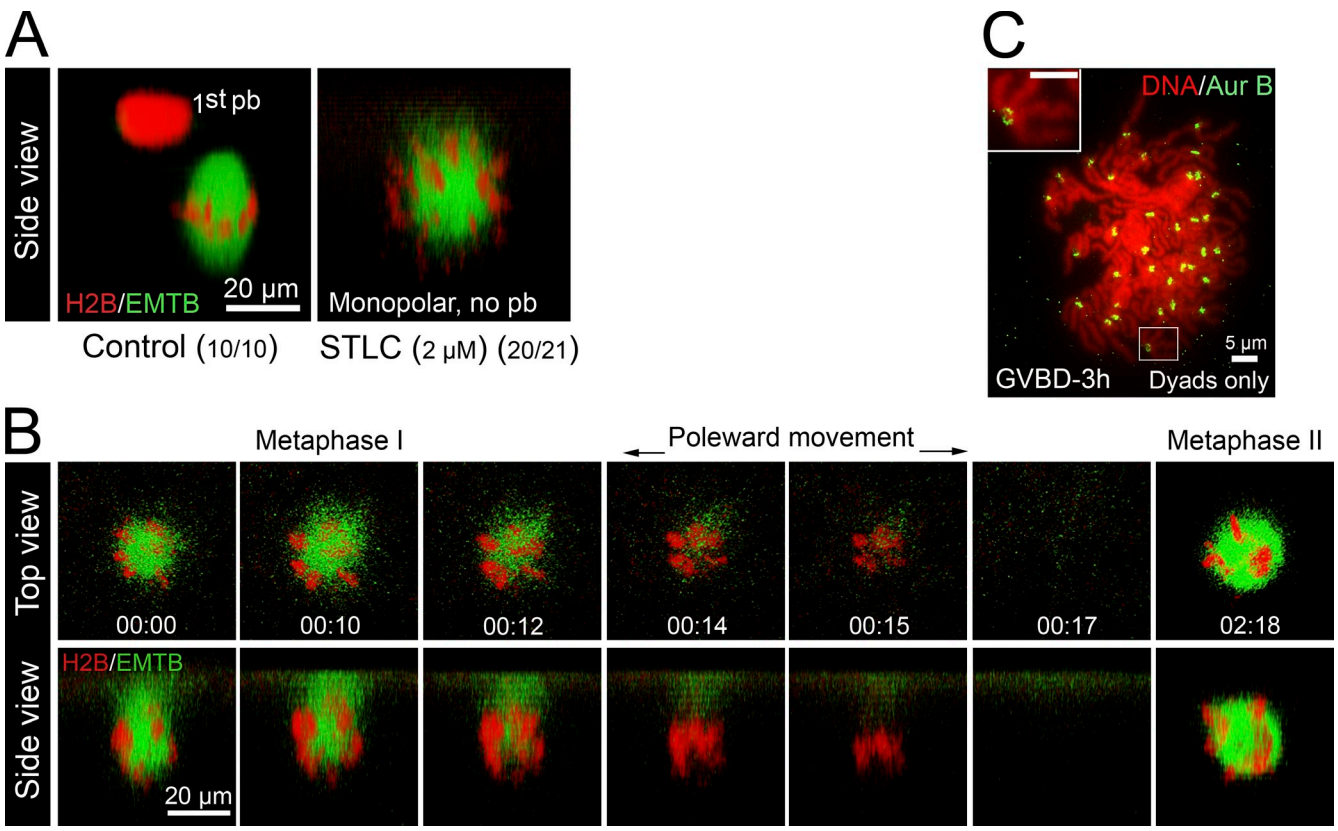

Figure 5. **Monopolar anaphase in STLC-treated oocytes.** (A) Oocytes injected with mChe-H2B and EMTB-3GFP were incubated overnight with progesterone (control) or progesterone plus 2 µM STLC. Oocytes were imaged live. Shown are representative images (side view) of a control oocyte (left) and an STLC-treated oocyte (right). (B) Time series of an STLC (2 µM)-treated oocyte during metaphase I–to–anaphase I transition (00:00–00:17), and arrested at metaphase II (02:18; $n = 5$). See Video 8 for the entire series. (C) Typical karyotype image of STLC-treated oocytes 3 h after GVBD. The inset depicts a dyad.

bivalent-to-dyad transition. Imaging these oocytes confirmed that no spindle microtubules were detectable and that chromosomes were aggregated at the cortex (Fig. 3 B, 00:00; also see Video 2). However, upon transfer to colcemid-free medium and UV exposure, a bipolar spindle gradually reformed, although typically with abnormalities including spindle asymmetry and chromosome misalignment (Fig. 3 B, 00:16). The reformed spindle would remain stable for as long as overnight (not depicted), which indicates that these oocytes were indeed arrested at metaphase II. To determine if these oocytes were capable of parthenogenetic activation, we pricked the oocyte (Leblanc et al., 2011). 12 min after pricking, anaphase occurred (Fig. 3 B, 00:28). This time course ($n = 10$) corresponds precisely to that found in control metaphase II eggs (Leblanc et al., 2011). Despite spindle abnormality and chromosome misalignment, the majority of these oocytes (8/10) successfully completed polar body emission (Fig. 3 B, 00:53). These results clearly indicate that in the absence of spindle microtubules, frog oocytes proceed to metaphase II.

Monopolar anaphase in *Xenopus* meiosis

We have recently shown that inhibition of Aur-B, by overexpressing Aur-B122R, in which the ATP-binding lysine-122 is replaced with arginine, results in monopolar meiosis I spindles in *Xenopus* oocytes (Shao et al., 2012). We reasoned that if frog oocytes do not have a functional SAC, these monopolar oocytes should undergo monopolar anaphase on time without additional intervention. Time-lapse imaging indicated that at the time (~120 min after GVBD) when control oocytes underwent anaphase and cytokinesis (Fig. 4 A, top, 00:04–00:18; also see Video 3), the Aur-B122R monopolar oocyte also exhibited apparent anaphase: microtubules rapidly disappeared, accompanied by chromosome aggregation indicative of poleward movement (Fig. 4 A, bottom, 00:14–00:17; also see Video 4) and by subsequent partial chromosome protrusion (Fig. 4 A, bottom, 00:26; see the cross-sectional view). However, the protrusion later retracted (Fig. 4 A, bottom, 00:32), with all chromosomes returning inside the oocyte to assemble another sphere-shape meiosis II spindle (Fig. 4 A, bottom, 00:52 and 01:06). Chromosome poleward movement was even more evident when control oocytes (Fig. 4 B, top, also see Video 5) and monopolar Aur-B122R oocytes (Fig. 4 B, bottom, also see Video 6) had been injected with Alexa Fluor 488 anti–Aur-A, which labels the spindle poles (Shao et al., 2012). Concurrent with chromosome poleward movement, Aur-B122R monopolar oocytes also exhibit prominent Cdc42 activation (see Video 7), as in control oocytes (Zhang et al., 2008).

In monopolar oocytes injected with Aur-B122R mRNA, chromosomes remained as bivalents in metaphase I (Fig. 4 C, top, 20/20). In contrast, when monopolar Aur-B122R oocytes

were analyzed 3 h or more after GVBD (metaphase II), we found only dyads (Fig. 4 C, middle, 18/18). When the Aur-B122R oocytes were karyotyped between 115 and 145 min after GVBD, 14% contained only bivalents and the remaining 86% contained only dyads (Fig. 4 D), which indicates that bivalent-to-dyad transition in Aur-B122R oocytes occurs at a similar time as in control oocytes (Fig. 1 B) or in nocodazole-treated oocytes (Fig. 2 C). Furthermore, when monopolar metaphase II oocytes were prick-activated, followed by karyotype analyses, we found only sister chromatids (Fig. 4 C, bottom, 9/9). Therefore, oocytes exhibiting monopolar spindles behaved similarly to their bipolar counterparts in undergoing bivalent-to-dyad transition in meiosis I and dyad-to-sister transition in meiosis II.

These results further support the notion that frog oocyte meiosis is not regulated by SAC. However, because Aur-B is thought to play a role in SAC signaling in mitosis (Musacchio and Salmon, 2007), an alternative interpretation might be that SAC is rendered inactive in Aur-B122R oocytes. To eliminate this possibility, we sought to generate monopolar spindles by inhibiting the Eg5 kinesin. We used S-trityl L-cysteine (STLC), a potent and specific inhibitor of Eg5 (Skoufias et al., 2006; Hu et al., 2008), after failing to generate monopolar meiosis I spindle using as much as 200 µM monastrol (unpublished data). Overnight incubation with STLC, at 2 µM (Fig. 5 A), or 10 or 50 µM (not depicted), consistently inhibited polar body emission and caused monopolar spindles. Time-lapse imaging indicated that ∼120 min after GVBD, spindle microtubules rapidly disappeared while chromosomes moved closer together (Fig. 5 B, 00:12–00:15, also see Video 8), which is suggestive of anaphase. We also observed the rapid disappearance of chromosomes from the cortical region (Fig. 5 B, 00:17); chromosomes only reappeared much later to assemble another monopolar spindle (Fig. 5 B, 02:18). This is in contrast to monopolar Aur-B122R oocytes in which the chromosomes remained at the cortex throughout meiosis I–to–meiosis II transition (Fig. 4). To confirm that these oocytes indeed underwent bivalent-to-dyad transition, we performed karyotype analyses of STLC-treated oocytes 3 h after GVBD (metaphase II in control oocytes) and found that these oocytes (11/11) contained ∼36 dyads (Fig. 5 C).

The lack of SAC is likely not restricted to meiosis in frog oocytes. It has been suggested that the meiosis in *Caenorhabditis elegans* oocytes also lacks SAC. Mutations in mei-1, mei-2, and zyg-9, which code for components of the oocyte spindle, do not cause metaphase arrest, even though spindles in these oocytes are severely abnormal (Clark-Maguire and Mains, 1994; Matthews et al., 1998). Similarly, mutations in multiple SAC genes do not affect cyclin B changes or chromosome segregation in *Drosophila melanogaster* oocytes (Batiha and Swan, 2012). However, direct demonstration that complete disruption of meiotic spindle does not cause metaphase arrest, as demonstrated here in frog oocytes, is lacking.

Interestingly, *Xenopus* embryos also appear to lack SAC during the cleavage stage of development (Murray and Kirschner, 1989). Therefore, embryos treated with high concentrations of nocodazole continue cycles of cyclin B degradation/resynthesis (Gerhart et al., 1984); embryos lacking any chromosomes (derived by artificial constriction of one cell embryo to produce a half embryo devoid of nucleus) continue cycles of cytokinesis-specific cortical contraction, in synchrony with control embryos (Hara et al., 1980). During mid-blastula transition in *Xenopus* embryos, when the cell cycle slows down and becomes asynchronous, SAC becomes evident (Clute and Masui, 1995). It seems likely that the loss of SAC occurs during oogenesis when the single egg cell becomes very large, and SAC reappears at mid-blastula embryos, when the blastomeres become much smaller.

Materials and methods

Oocytes preparation, microinjection, and drug treatment

Sexually mature *Xenopus* females were purchased from Nasco. Ovaries were obtained from *Xenopus* within 3–10 d after injection of PMSG. Oocytes were manually defolliculated (Liu and Liu, 2006) and were kept at 18°C in oocyte culture medium (OCM; 60% of L-15 medium [Sigma-Aldrich], supplemented with 1.07 g BSA per liter, mixed with 40% autoclaved water to yield the appropriate isotonic solution for amphibian oocytes). Defolliculated oocytes were injected with mRNA encoding various probes. Plasmids encoding pCS2-mChe-H2B, pCS2-EMTB-3GFP (von Dassow G. et al., 2009), and pCS2-EGFP-wGBD (Benink and Bement, 2005) were provided by W.M. Bement (University of Wisconsin, Madison, Madison, WC). The plasmid encoding pRN3-β5-tubulin-GFP (Verlhac et al., 2000) was provided by M.-H. Verlhac (Collège de France, Paris, France). The plasmid pSP64TM-AurB122R encodes *Xenopus* Aur-B with a single amino acid substitution, codon AAG (Lys-122) replaced by AGG (Arg), and has been described previously (Shao et al., 2012). The plasmid pCS2+HA-Securin dm encodes a nondestructible mutant of *Xenopus* securin (Zou et al., 1999), and has been described previously (Zhang et al., 2008). Oocytes injected with mRNA were incubated in OCM for at least 6 h before the addition of 1 µM progesterone to induce oocyte maturation. Oocytes were monitored for GVBD (indicated by the appearance of a white maturation spot) every 10 min. GVBD oocytes were individually transferred to fresh OCM without progesterone and further incubated, until the time of fluorescence imaging or derivation of mini-cells for chromosome analyses.

Nocodazole (M1404; Sigma-Aldrich) stock solution was prepared at 3.3 mM in DMSO and stored at −20°C. The stock was added directly to OCM at the indicated time to a final concentration of 3.3 µM. Colcemid (D7385; Sigma-Aldrich) stock solution was prepared at 50 mM in DMSO and stored at −20°C. The stock was added directly to OCM to a final concentration of 50 µM 30 min after GVBD. 3 h after GVBD (when control oocytes were at metaphase II), the colcemid-treated eggs were transferred to colcemid-free oocyte incubation medium (OR2) and exposed to UV excitation through a 60× oil objective lens (11000V3 [Chroma]; 350/50 nm; 100-W mercury bulb) and simultaneously subjected to confocal imaging. After a bipolar spindle emerged, the oocyte was pricked by a glass needle (Leblanc et al., 2011), and the UV exposure and imaging continued.

STLC (2799-0707; Tocris Bioscience) stock solution was prepared at 50 mM in DMSO and stored at −20°C. STLC (2–50 µM) was added to OCM together with 1 µM progesterone to germinal vesicles oocytes. STLC was present throughout the whole experiment, including in the imaging chamber.

Live cell imaging and image processing

Although individual oocytes vary, often considerably, in the timing of GVBD after the addition of progesterone, we found that they are remarkably synchronized from GVBD to first polar body emission (Ma et al., 2006; Zhang et al., 2008). Typically, 120 min after GVBD, the oocyte initiates anaphase I. In all figures, time zero (00:00) corresponds to the start of the imaging of the particular oocyte, not GVBD time. Oocytes were imaged with a 60× oil objective lens on an inverted microscope (Axiovert; Carl Zeiss) with a laser scanning confocal imaging system (1024; Bio-Rad Laboratories), equipped with a krypton argon ion laser. Green fluorophores (EGFP fusion proteins or Alexa Fluor 488–coupled antibodies) were excited with a 488-nm laser line, coupled with a 522/35 emission filter, and red fluorophores (RFP fusion proteins) were excited with a 568-nm line, coupled with a 605/32 emission filter. Time-lapse image series were collected at various time intervals. Each time point volume was comprised of 15–25 image planes, 1–2 µm apart (z step). Image series were rendered in 3D using Volocity Visualization software (PerkinElmer). Most of the

time series in this paper are 3D images in the transverse direction ("side view") such that the readers are looking "side-on" at the plasma membrane. "Top view" refers to the direct view as seen through the microscope eye piece.

Analyzing chromosome karyotypes during *Xenopus* oocyte maturation

Frog oocytes were incubated in OR2 (83 mM NaCl, 2.5 mM KCl, 1 mM $CaCl_2$, 1 mM $MgCl_2$, 1 mM Na_2HPO_4, and 5 mM Hepes, pH 7.8) containing 10 µg/ml cytochalasin B and 1 mg/ml BSA for 10 min before the vitelline envelope was torn off using a pair of fine forceps. A glass needle with an inner diameter of 70 µm was placed over the translucent spot (spindle anchoring site; Fig. 1 A), and negative pressure was applied to the needle, using a microinjector (100; Medical System). When the translucent spot was found to have entered the needle tip, negative pressure was stopped and the oocyte was gently moved to sever a mini-cell. The mini-cell was expelled into the dish by applying positive pressure, and was immediately transferred into 1 mg/ml BSA in water (hypotonic solution). 10 min later, the mini-cell was carefully transferred onto a glass slide prewet with fixative (1% paraformaldehyde in water, pH 9.2, containing 0.15% Triton X-100 and 3 mM dithiothreitol). The slide was kept in a humid box overnight before air-drying for 1–2 h. The slide was carefully rinsed in 0.4% Photoflo (Kodak) in double-distilled H_2O, and air-dried at room temperature (Hodges and Hunt, 2002). The slides were then subjected to immunostaining with antibodies against Aur-B (Zhang et al., 2008; Shao et al., 2012) and counterstained with Sytox orange (Invitrogen). Chromosomes and chromosome-associated Aur-B were visualized by epifluorescence microscopy, using an inverted microscope (1X70; Olympus) with either 60×/1.35 oil objective or 40×/0.95 objective lenses. Images were acquired with a digital camera (FC sin 00170121; Lumenera), operated with the Infinity program. The double-stained images were merged with Volocity, with no further manipulations.

Online supplemental material

Fig. S1 represents nocodazole-treated oocytes immunostained with anti-tubulin antibodies to complement time-lapse imaging data in Fig. 2 A. Fig. S2 depicts nocodazole-treated mouse oocytes undergoing metaphase I arrest with chromosome bivalents. There are also seven videos (Videos 1–6 and 8) corresponding, respectively, to Fig. 2 A, Fig. 3 B, Fig. 4 A (top), Fig. 4 A (bottom), Fig. 4 B (top), Fig. 4 B (bottom), and Fig. 5 B. Video 7 depicts an Aur-B122R monopolar oocyte undergoing Cdc42 activation, concurrent with monopolar anaphase. Online supplemental material is available at http://www.jcb.org/cgi/content/full/jcb.201211041/DC1. Additional data are available in the JCB DataViewer at http://dx.doi.org/10.1083/jcb.201211041.dv.

We thank Drs. William Bement and Marie-Helene Verlhac for plasmids.

This work is supported by an operating grant from the Canadian Institute of Health Research (MOP89973).

Submitted: 6 November 2012
Accepted: 11 March 2013

References

Batiha, O., and A. Swan. 2012. Evidence that the spindle assembly checkpoint does not regulate APC(Fzy) activity in *Drosophila* female meiosis. *Genome*. 55:63–67. http://dx.doi.org/10.1139/g11-079

Bayaa, M., R.A. Booth, Y. Sheng, and X.J. Liu. 2000. The classical progesterone receptor mediates *Xenopus* oocyte maturation through a nongenomic mechanism. *Proc. Natl. Acad. Sci. USA*. 97:12607–12612. http://dx.doi.org/10.1073/pnas.220302597

Belloc, E., and R. Méndez. 2008. A deadenylation negative feedback mechanism governs meiotic metaphase arrest. *Nature*. 452:1017–1021. http://dx.doi.org/10.1038/nature06809

Benink, H.A., and W.M. Bement. 2005. Concentric zones of active RhoA and Cdc42 around single cell wounds. *J. Cell Biol.* 168:429–439. http://dx.doi.org/10.1083/jcb.200411109

Brunet, S., A.S. Maria, P. Guillaud, D. Dujardin, J.Z. Kubiak, and B. Maro. 1999. Kinetochore fibers are not involved in the formation of the first meiotic spindle in mouse oocytes, but control the exit from the first meiotic M phase. *J. Cell Biol.* 146:1–12. http://dx.doi.org/10.1083/jcb.146.1.1

Clark-Maguire, S., and P.E. Mains. 1994. Localization of the mei-1 gene product of *Caenorhaditis elegans*, a meiotic-specific spindle component. *J. Cell Biol.* 126:199–209. http://dx.doi.org/10.1083/jcb.126.1.199

Clute, P., and Y. Masui. 1995. Regulation of the appearance of division asynchrony and microtubule-dependent chromosome cycles in *Xenopus laevis* embryos. *Dev. Biol.* 171:273–285. http://dx.doi.org/10.1006/dbio.1995.1280

Eichenlaub-Ritter, U., and I. Boll. 1989. Nocodazole sensitivity, age-related aneuploidy, and alterations in the cell cycle during maturation of mouse oocytes. *Cytogenet. Cell Genet.* 52:170–176. http://dx.doi.org/10.1159/000132871

Ferrell, J.E. Jr., and E.M. Machleder. 1998. The biochemical basis of an all-or-none cell fate switch in *Xenopus* oocytes. *Science*. 280:895–898. http://dx.doi.org/10.1126/science.280.5365.895

Furuno, N., M. Nishizawa, K. Okazaki, H. Tanaka, J. Iwashita, N. Nakajo, Y. Ogawa, and N. Sagata. 1994. Suppression of DNA replication via Mos function during meiotic divisions in *Xenopus* oocytes. *EMBO J.* 13:2399–2410.

Gall, J.G., and Z. Wu. 2010. Examining the contents of isolated *Xenopus* germinal vesicles. *Methods*. 51:45–51. http://dx.doi.org/10.1016/j.ymeth.2009.12.010

Gerhart, J., M. Wu, and M. Kirschner. 1984. Cell cycle dynamics of an M-phase-specific cytoplasmic factor in *Xenopus laevis* oocytes and eggs. *J. Cell Biol.* 98:1247–1255. http://dx.doi.org/10.1083/jcb.98.4.1247

Graf, J.-D., and H.R. Kobel. 1991. Genetics of *Xenopus laevis*. *Methods Cell Biol.* 36:19–34. http://dx.doi.org/10.1016/S0091-679X(08)60270-8

Hara, K., P. Tydeman, and M. Kirschner. 1980. A cytoplasmic clock with the same period as the division cycle in *Xenopus* eggs. *Proc. Natl. Acad. Sci. USA*. 77:462–466. http://dx.doi.org/10.1073/pnas.77.1.462

Hodges, C.A., and P.A. Hunt. 2002. Simultaneous analysis of chromosomes and chromosome-associated proteins in mammalian oocytes and embryos. *Chromosoma*. 111:165–169. http://dx.doi.org/10.1007/s00412-002-0195-3

Homer, H.A., A. McDougall, M. Levasseur, A.P. Murdoch, and M. Herbert. 2005. Mad2 is required for inhibiting securin and cyclin B degradation following spindle depolymerisation in meiosis I mouse oocytes. *Reproduction*. 130:829–843. http://dx.doi.org/10.1530/rep.1.00856

Hu, C.K., M. Coughlin, C.M. Field, and T.J. Mitchison. 2008. Cell polarization during monopolar cytokinesis. *J. Cell Biol.* 181:195–202. http://dx.doi.org/10.1083/jcb.200711105

Kolano, A., S. Brunet, A.D. Silk, D.W. Cleveland, and M.H. Verlhac. 2012. Error-prone mammalian female meiosis from silencing the spindle assembly checkpoint without normal interkinetochore tension. *Proc. Natl. Acad. Sci. USA*. 109:E1858–E1867. http://dx.doi.org/10.1073/pnas.1204686109

Leblanc, J., X. Zhang, D. McKee, Z.B. Wang, R. Li, C. Ma, Q.Y. Sun, and X.J. Liu. 2011. The small GTPase Cdc42 promotes membrane protrusion during polar body emission via ARP2-nucleated actin polymerization. *Mol. Hum. Reprod.* 17:305–316. http://dx.doi.org/10.1093/molehr/gar026

LeMaire-Adkins, R., K. Radke, and P.A. Hunt. 1997. Lack of checkpoint control at the metaphase/anaphase transition: a mechanism of meiotic nondisjunction in mammalian females. *J. Cell Biol.* 139:1611–1619. http://dx.doi.org/10.1083/jcb.139.7.1611

Liu, X.S., and X.J. Liu. 2006. Oocyte isolation and enucleation. *Methods Mol. Biol.* 322:31–41. http://dx.doi.org/10.1007/978-1-59745-000-3_3

Ma, C., C. Cummings, and X.J. Liu. 2003. Biphasic activation of Aurora-A kinase during the meiosis I- meiosis II transition in *Xenopus* oocytes. *Mol. Cell. Biol.* 23:1703–1716. http://dx.doi.org/10.1128/MCB.23.5.1703-1716.2003

Ma, C., H.A. Benink, D. Cheng, V. Montplaisir, L. Wang, Y. Xi, P.P. Zheng, W.M. Bement, and X.J. Liu. 2006. Cdc42 activation couples spindle positioning to first polar body formation in oocyte maturation. *Curr. Biol.* 16:214–220. http://dx.doi.org/10.1016/j.cub.2005.11.067

Matthews, L.R., P. Carter, D. Thierry-Mieg, and K. Kemphues. 1998. ZYG-9, a *Caenorhabditis elegans* protein required for microtubule organization and function, is a component of meiotic and mitotic spindle poles. *J. Cell Biol.* 141:1159–1168. http://dx.doi.org/10.1083/jcb.141.5.1159

Murray, A.W., and M.W. Kirschner. 1989. Dominoes and clocks: the union of two views of the cell cycle. *Science*. 246:614–621. http://dx.doi.org/10.1126/science.2683077

Musacchio, A., and E.D. Salmon. 2007. The spindle-assembly checkpoint in space and time. *Nat. Rev. Mol. Cell Biol.* 8:379–393. http://dx.doi.org/10.1038/nrm2163

Nagaoka, S.I., C.A. Hodges, D.F. Albertini, and P.A. Hunt. 2011. Oocyte-specific differences in cell-cycle control create an innate susceptibility to meiotic errors. *Curr. Biol.* 21:651–657. http://dx.doi.org/10.1016/j.cub.2011.03.003

Ohan, N., Y. Agazie, C. Cummings, R. Booth, M. Bayaa, and X.J. Liu. 1999. RHO-associated protein kinase α potentiates insulin-induced MAP kinase activation in *Xenopus* oocytes. *J. Cell Sci.* 112:2177–2184.

Ohsumi, K., W. Sawada, and T. Kishimoto. 1994. Meiosis-specific cell cycle regulation in maturing *Xenopus* oocytes. *J. Cell Sci.* 107:3005–3013.

Peter, M., A. Castro, T. Lorca, C. Le Peuch, L. Magnaghi-Jaulin, M. Dorée, and J.C. Labbé. 2001. The APC is dispensable for first meiotic anaphase in *Xenopus* oocytes. *Nat. Cell Biol.* 3:83–87. http://dx.doi.org/10.1038/35050607

Pines, J. 2006. Mitosis: a matter of getting rid of the right protein at the right time. *Trends Cell Biol.* 16:55–63. http://dx.doi.org/10.1016/j.tcb.2005.11.006

Rieder, C.L., A. Schultz, R. Cole, and G. Sluder. 1994. Anaphase onset in vertebrate somatic cells is controlled by a checkpoint that monitors sister kinetochore attachment to the spindle. *J. Cell Biol.* 127:1301–1310. http://dx.doi.org/10.1083/jcb.127.5.1301

Rieder, C.L., R.W. Cole, A. Khodjakov, and G. Sluder. 1995. The checkpoint delaying anaphase in response to chromosome monoorientation is mediated by an inhibitory signal produced by unattached kinetochores. *J. Cell Biol.* 130:941–948. http://dx.doi.org/10.1083/jcb.130.4.941

Schultz, R.M., and P.M. Wassarman. 1977. Biochemical studies of mammalian oogenesis: Protein synthesis during oocyte growth and meiotic maturation in the mouse. *J. Cell Sci.* 24:167–194.

Shao, H., C. Ma, X. Zhang, R. Li, A.L. Miller, W.M. Bement, and X.J. Liu. 2012. Aurora B regulates spindle bipolarity in meiosis in vertebrate oocytes. *Cell Cycle*. 11:2672–2680. http://dx.doi.org/10.4161/cc.21016

Skoufias, D.A., S. DeBonis, Y. Saoudi, L. Lebeau, I. Crevel, R. Cross, R.H. Wade, D. Hackney, and F. Kozielski. 2006. S-trityl-L-cysteine is a reversible, tight binding inhibitor of the human kinesin Eg5 that specifically blocks mitotic progression. *J. Biol. Chem.* 281:17559–17569. http://dx.doi.org/10.1074/jbc.M511735200

Sluder, G. 1979. Role of spindle microtubules in the control of cell cycle timing. *J. Cell Biol.* 80:674–691. http://dx.doi.org/10.1083/jcb.80.3.674

Soewarto, D., H. Schmiady, and U. Eichenlaub-Ritter. 1995. Consequences of non-extrusion of the first polar body and control of the sequential segregation of homologues and chromatids in mammalian oocytes. *Hum. Reprod.* 10:2350–2360.

Taieb, F.E., S.D. Gross, A.L. Lewellyn, and J.L. Maller. 2001. Activation of the anaphase-promoting complex and degradation of cyclin B is not required for progression from Meiosis I to II in *Xenopus* oocytes. *Curr. Biol.* 11:508–513. http://dx.doi.org/10.1016/S0960-9822(01)00145-2

Tian, J., S. Kim, E. Heilig, and J.V. Ruderman. 2000. Identification of XPR-1, a progesterone receptor required for *Xenopus* oocyte activation. *Proc. Natl. Acad. Sci. USA*. 97:14358–14363. http://dx.doi.org/10.1073/pnas.250492197

Verlhac, M.H., C. Lefebvre, P. Guillaud, P. Rassinier, and B. Maro. 2000. Asymmetric division in mouse oocytes: with or without Mos. *Curr. Biol.* 10:1303–1306. http://dx.doi.org/10.1016/S0960-9822(00)00753-3

von Dassow, G., K.J. Verbrugghe, A.L. Miller, J.R. Sider, and W.M. Bement. 2009. Action at a distance during cytokinesis. *J. Cell Biol.* 187:831–845. http://dx.doi.org/10.1083/jcb.200907090

Wassarman, P.M., W.J. Josefowicz, and G.E. Letourneau. 1976. Meiotic maturation of mouse oocytes in vitro: inhibition of maturation at specific stages of nuclear progression. *J. Cell Sci.* 22:531–545.

Zhang, X., C. Ma, A.L. Miller, H.A. Katbi, W.M. Bement, and X.J. Liu. 2008. Polar body emission requires a RhoA contractile ring and Cdc42-mediated membrane protrusion. *Dev. Cell*. 15:386–400. http://dx.doi.org/10.1016/j.devcel.2008.07.005

Zou, H., T.J. McGarry, T. Bernal, and M.W. Kirschner. 1999. Identification of a vertebrate sister-chromatid separation inhibitor involved in transformation and tumorigenesis. *Science*. 285:418–422. http://dx.doi.org/10.1126/science.285.5426.418